Synthesis, Crystal Structures, and Second-Order Nonlinear Optical Properties of New Chiral Ferrocenyl Materials

Gilbert G. A. Balavoine,* Jean-Claude Daran, Gabriel Iftime, Pascal G. Lacroix,* and Eric Manoury*

Laboratoire de Chimie de Coordination, 205 route de Narbonne, F-31077 Toulouse Cedex, France

Jacques A. Delaire, Isabelle Maltey-Fanton, and Keitaro Nakatani

PPSM, CNRS UA 1906, Ecole Normale Supérieure de Cachan, Avenue du President Wilson, 94235 Cachan Cedex, France

Santo Di Bella

Dipartimento di Scienze Chimiche, Università di Catania, 95125 Catania, Italy

Received October 5, 1998

A series of chiral enantiomerically pure analogues of (*E*)-(2-(4-nitrophenyl)ethenyl)ferrocene (**2**), substituted by R (**3**, R = Me; **4**, R = CH_2OH; **5**, R = $SiMe_3$), in the 2-position on the cyclopentadienyl ring, were synthesized. Measurements by electric-field-induced second-harmonic generation (EFISH) and calculations by INDOS/CI-SOS show that the different chromophores have closely related molecular NLO responses. However, the crystal packings for the different compounds, observed by X-ray diffraction on a monocrystal, are completely different. In any case, the chirality of the constituting molecules avoids the centrosymmetry of the crystals and therefore preserves the NLO efficiency in the solid state. In the case of **3**, the crystal packing is close to the centrosymmetry and so the bulk NLO efficiency is low (6 times that of urea, $\lambda = 1.907$ μm) but not nil, as is the case for **2**. For **4**, the crystal packing is much better for NLO (efficiency 20 times that of urea, $\lambda = 1.907$ μm) and is almost optimized for **5** (efficiency 100 times that of urea, $\lambda = 1.907$ μm). The correlation between molecular and bulk NLO responses was studied using the model proposed by Zyss.

Introduction

These last two decades, molecular-based second-order nonlinear optical (NLO) chromophores have attracted much interest because of their potential applications in emerging optoelectronic technologies.[1−3] These efforts have mainly focused on organic systems.[1−4] More recently, organometallic molecules have been investigated as well.[5−11] In comparison to common organic molecules, they offer a larger variety of novel structures, the possibility of high environmental stability, and a diversity of tunable electronic behaviors by virtue of the coordinated metal center which might bring about NLO materials with unique characteristics such as magnetic and electrochemical properties.[12,13] The report in 1987 by Green et al.[14] that the ferrocene complex (*Z*)-1-ferrocenyl-2-(4-nitrophenyl)ethylene (**1**; Chart 1) had SHG efficiency 62 times that of urea first demonstrated

* To whom correspondence should be addressed. Tel: (33) 5 61 33 31 73. Fax: (33) 5 61 33 31 31. E-mail: G.G.A.B., balavoin@lcc-toulouse.fr; P.G.L., pascal@lcc-toulouse.fr; E.M., manoury@lcc-toulouse.fr.

(1) (a) *Molecular Nonlinear Optics*; Zyss, J., Ed.; Academic Press: New York, 1994. (b) *Nonlinear Optical Properties of Organic Molecules and Crystals*; Chemla, D. S., Zyss, J., Eds.; Academic Press: New York, 1987; Vols. 1 and 2. (c) Prasad, N. P.; Williams, D. J. *Introduction to Nonlinear Optical Effects in Molecules and Polymers*; Wiley: New York, 1991.

(2) *Proc. SPIE-Int. Soc. Opt. Eng.* **1988,** *971*; **1989**, *1147*; **1990**, *1337*; **1991**, *1560*; **1992**, *1775*; **1993**, *2025*, **1994**, *2285*.

(3) For recent reviews see: (a) Dalton, L. R.; Harper, A. W.; Ghosn, R.; Steier, W. H.; Ziari, M.; Fetterman, H.; Shi, Y.; Mustacich, R. V.; Jen, A. K. Y.; Shea, K. J. *Chem. Mater.* **1995**, *7*, 1060−1081. (b) Denning, R. G. *J. Mater. Chem.* **1995**, *5*, 365−378. (c) Burland, D. M. Optical Nonlinearities in Chemistry. *Chem. Rev.* **1994**, *94*, 1−2. (d) Marder, S. R.; Beratan, D. N.; Cheng, L. T.; *Science* **1991**, *252*, 103−106.

(4) Among recent reports on organic chromophores with enhanced nonlinearity, see for example: (a) Blanchard-Desce, M.; Alain, V.; Bedworth, P. V.; Marder, S. R.; Fort, A.; Runser, C.; Barzoukas, M.; Lebus, S.; Wortmann, R. *Chem. Eur. J.* **1997**, *3*, 1091−1104. (b) Rao, V. P.; Jen, A. K.-Y.; Wong, K. Y.; Drost, K. J. *J. Chem. Soc., Chem. Commun.* **1993**, 1118−1120. (c) Pushkana Rao, V.; Jen, A. K.-Y.; Chandrasekhar, J.; Namboothiri, I. N. N.; Rathna, A. *J. Am. Chem. Soc.* **1996**, *118*, 12443−12448. (d) Marder, S. R.; Cheng, L. T.; Tiemann, B. G.; Friedli, A. C.; Blanchard-Desce, M.; Perry, J. W.; Skindhoj, J. *Science* **1994**, *263*, 511−514. (e) Gilmour, S.; Montgomery, R. A.; Marder, S. R.; Cheng, L.-T.; Jen, A. K.-Y.; Cai, Y.; Perry, J. W.; Dalton, L. R. *Chem. Mater.* **1994**, *6*, 1603−1604.

(5) For recent reviews on NLO organometallics see: (a) Long, N. J. *Angew. Chem., Int. Ed. Engl.* **1995**, *34*, 21−38. (b) Marder, S. R. In *Inorganic Materials*; Bruce, D. W., O'Hare, D., Eds.; Wiley: New York, 1992; pp 115−164. (c) Whittall, I. R.; McDonagh, A. M.; Humphrey, M. G. *Adv. Organomet. Chem.* **1998**, *42*, 291−357.

(6) (a) Whittall, I. R.; Humphrey, M. G.; Houbrechts, S.; Persoons, A.; Hockless, D. C. R. *Organometallics* **1996**, *15*, 5738−5745. (b) Whittall, I. R.; Humphrey, M. G.; Hockless, D. C. R.; Skelton, B. W.; White, A. H. *Organometallics* **1995**, *14*, 3970−3979.

(7) (a) Kanis, D. R.; Lacroix, P. G.; Ratner, M. A.; Marks, T. J. *J. Am. Chem. Soc.* **1994**, *116*, 10089−10102. (b) Kanis, D. R.; Ratner, M. A.; Marks, T. J. *J. Am. Chem. Soc.* **1992**, *114*, 10338−10357.

10.1021/om980826y CCC: $18.00
Publication on Web 12/09/1998

Chart 1

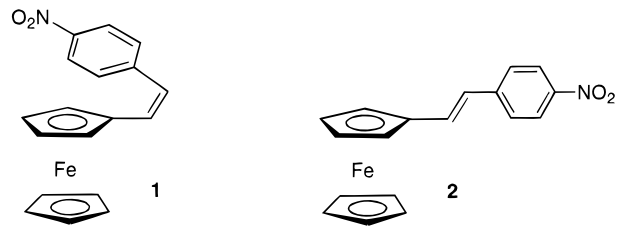

that organometallic compounds, in particular metallocenes, could exhibit large efficiencies. To date, ferrocene-based donor−acceptor materials are still the most efficient SHG organometallic compounds.[15] Nevertheless, the main bottleneck to the development of second-order NLO material is the compulsory noncentrosymmetric environment of the chromophores if the molecular hyperpolarizability (β) is to contribute to an observable bulk nonlinear susceptibility (χ^2).[4] For example, the *cis*-ferrocene derivative **1** exhibits a modest β value of 13×10^{-30} esu but a large bulk efficiency (62 times that of urea) due to its noncentrosymmetric crystal structure, while the *trans* isomer **2** (see Chart 1), which possesses a larger hyperpolarizability at the molecular level ($\beta = 31 \times 10^{-30}$ esu), is not efficient in the solid state due to its probable centrosymmetry.[16,14]

The present paper reports on the engineering of this promising ferrocenyl-based molecule **2** into a noncentrosymmetric environment. An established strategy to achieve this goal is chirality.[17] Recently an efficient synthesis of various enantiomerically pure 2-substituted ferrocenecarbaldehydes was developed.[18] We thought that this new method could provide us various chiral enantiomerically pure 2-substituted analogues of **2** and hence an opportunity to study the influence of the substituents in the 2-position on the NLO properties. Therefore, we decided to prepare different chromophores with substituents of different sizes and different abilities for hydrogen bonding (see Scheme 1). Our study focuses on the synthesis, crystal structure, linear optical spectroscopy, powder efficiency second-harmonic generation (SHG),[19] and hyperpolarizability measurements by the electric-field-induced second-harmonic generation (EFISH) technique,[20] in combination with a quantum chemical analysis, within the proven INDO/S-SOS (ZINDO) formalism,[21,22] to describe the structure NLO property relationships of some of these chiral enantiomerically pure organometallic NLO chromophores **3**−**5**.

Experimental Section

Synthesis. All reactions were carried out in the absence of air using standard Schlenk techniques and vacuum-line manipulations. Iodomethane, chlorotrimethylsilane, and dimethylformamide were freshly distilled on calcium hydride prior to use. Other compounds were used without further purification. All solvents were dried before use. Thin-layer chromatography was carried out on Merck Kieselgel $60F_{254}$ precoated silica gel plates. Preparative flash chromatography was performed on Merck Kieselgel. Instrumentation: Bruker AM250 (^{1}H, ^{13}C NMR), Hewlett-Packard HP MSD 7590 (GC/MS), Hewlett-Packard HP 8452A (UV−vis), Perkin-Elmer 1725X (FT-IR), Perkin-Elmer 241 (polarimeter). Elemental analyses were performed by the Service d'Analyse du Laboratoire de Chimie de Coordination, Toulouse, France.

(4-Nitrobenzyl)triphenylphosphonium bromide was synthesized by a similar procedure described in ref 23 for the synthesis of (4-nitrobenzyl)triphenylphosphonium chloride. **7a**−**c** and **8a**,**b** were synthesized according to ref 18a. The physical data of **8a**, **7b** and **8b**, and **7c** are identical with those reported respectively in ref 24, 18b, and 25.

(2*S*,4*S*,*R*$_{Fc}$)-4-(Methoxymethyl)-2-(2-methylferrocenyl)-1,3-dioxane 7a. ^{1}H NMR ($CDCl_3$; δ (ppm)): 5.45 (s, 1H, O−CH−O); 4.25 (m, 3H, 1H C_5H_3 and 2H CH−O); 4.06 (s, 5H, C_5H_5); 4.01 (m, 1H, C_5H_3); 3.98 (m, 2H, 1H C_5H_3 and 1H CH−O); 3.49 (dd, J = 10.1 and 6.0 Hz, AB, 1H, CH_2−O); 3.37 (s, 3H, $-OCH_3$); 3.35 (br dd, J = 10.1 and 5.5 Hz, AB, 1H, CH_2−O), 2.02 (s, 3H, CH_3), 1.76 (br qd, J = 12.2 Hz and 5.1 Hz, CH_2), 1.47 (br dd, J_{gem} = 13.2 and 1.1 Hz, CH_2). GC-MS (IE, 70 eV; *m/e*): 331 (M + 1, 21%); 330 (M, 100%); 228 (16%); 121 (13%); 56 (14%). $[\alpha]_D = -41.7$ ($CHCl_3$, c = 0.83). Anal. Calcd for $C_{17}H_{22}FeO_3$: C, 61.82; H, 6.67. Found: C, 62.14; H, 6.97.

Wittig Reaction (General Procedure). tBuOK (3 equiv) and (4-nitrobenzyl)triphenylphosphonium bromide (2.5 equiv) were added into a distillation apparatus. The system was purged with argon. Dry toluene (10 mL/mmol of phosphonium) was added to the mixture of solids. The mixture was warmed. After 1 h, 6 mL of toluene was removed by distillation and

(8) (a) Coe, B. J.; Hamor, T. A.; Jones, C. J.; McCleverty, J. A.; Bloor, D.; Cross, G. H.; Axon, T. L. *J. Chem. Soc., Dalton Trans.* **1995**, 673−684. (b) Coe, B. J.; Foulon, J. D.; Hamor, T. A.; Jones, C. J.; McCleverty, J. A.; Bloor, D.; Cross, G. H.; Axon, T. L. *J. Chem. Soc., Dalton Trans.* **1994**, 3427−3439. (c) Houlton, A.; Jasim, N.; Roberts, R. M. G.; Silver, J.; Cunningham, D.; Mcardle, P.; Higgins, T. *J. Chem. Soc., Dalton Trans.* **1992**, 2235−2241.

(9) (a) Doisneau, G.; Balavoine, G.; Fillebeen-Khan, T.; Clinet, J.-C.; Delaire, J. A.; Ledoux, I.; Loucif, R.; Puccetti, G. *J. Organomet. Chem.* **1991**, *421*, 299−304. (b) Loucif-Saïbi, R.; Delaire, J. A.; Bonazzola, L.; Doisneau, G.; Balavoine, G.; Fillebeen-Khan, T.; Ledoux, I.; Puccetti, G. *Chem. Phys.* **1992**, *167*, 369−375.

(10) (a) Wright, M. E.; Toplikar, E. G.; Lackritz, H. S.; Kerney, J. T. *Macromolecules* **1994**, *27*, 3016−3022. (b) Wright, M. E.; Toplikar, E. G. *Macromolecules* **1992**, *25*, 6050−6054. (c) Wright, M. E.; Sigman, M. S. *Macromolecules* **1992**, *25*, 6055−6058.

(11) Cheng, L. T.; Tam, W.; Meredith, G. R.; Marder, S. R. *Mol. Cryst. Liq. Cryst.* **1990**, *189*, 137−153.

(12) (a) Geoffroy, G. L.; Wrighton, M. S. *Orgonometallic Photochemistry*; Academic Press: New York, 1979. (b) Collman, J. P.; Hegedus, L. S. *Principles and Applications of Organotransition Metal Chemistry*; University Science Books: Mill Valley, CA, 1987.

(13) Kahn, O. *Molecular Magnetism*; VCH: New York, 1993.

(14) Green, M. L. H.; Marder, S. R.; Thompson, M. E.; Bandy, J. A.; Bloor, D.; Kolinsky, P. V.; Jones, R. J. *Nature* **1987**, *330*, 360−362.

(15) Marder, S. R.; Perry, J. W.; Schaefer, W. P.; Tiemann, B. G. *Organometallics* **1991**, *10*, 1896−1901.

(16) Calabrese, J. C.; Cheng, L.-T.; Green, J. C.; Marder, S. R.; Tam, W. *J. Am. Chem. Soc.* **1991**, *113*, 7227−7232.

(17) See for example: (a) Zyss, J.; Nicoud, J. F.; Coquillay *J. Chem. Phys.* **1984**, *81*, 4160−4167. (b) Oudar, J. L.; Hierle, R. *J. Appl. Phys.* **1977**, *48*, 2699−2704.

(18) (a) Riant, O.; Samuel, O.; Kagan, H. B. *J. Am. Chem. Soc.* **1993**, *115*, 5835−5836. (b) Riant, O.; Samuel, O.; Flessner, T.; Taudien, S.; Kagan, H. B. *J. Org. Chem.* **1997**, *62*, 6733−6745.

(19) (a) Kurtz, S. K.; Perry, T. T. *J. Appl. Phys.* **1968,** *39*, 3798−3813. (b) Dougherty, J. P.; Kurtz, S. K. *J. Appl. Crystallogr.* **1976**, *9*, 145−158.

(20) For a general discussion of the EFISH technique, see: (a) Oudar, J. L. *J. Chem. Phys.* **1977**, *67*, 446−457. (b) Levine, B. F.; Betha, C. G. *J. Chem. Phys.* **1976**, *65*, 2429−2438. (b) Levine, B. F.; Betha, C. G. *J. Chem. Phys.* **1976**, *65*, 2439−2442.

(21) (a) Di Bella, S.; Fragalà, I.; Marks, T. J.; Ratner, M. A. *J. Am. Chem. Soc.* **1996**, *118*, 8, 12747−12751. (b) Kanis, D. R.; Ratner, M. A.; Marks, T. J. *Chem. Rev.* **1994**, *94*, 195−242.

(22) (a) There are several definitional issues associated with comparing calculated microscopic responses to those obtained by experiment.[22b] In the present contribution, both derived theoretical and experimental $\beta\mu$ values employ the Ward definition,[22c] within a perturbation series expansion. (b) Willetts, A.; Rice, J. E.; Burland, D. M.; Shelton, D. P. *J. Chem. Phys.* **1992**, *97*, 7590−7599. (c) Ward, J. F. *Rev. Mod. Phys.* **1965**, *37*, 1−18.

(23) Ketcham, R.; Jamboktar, D.; Martinelli, L. *J. Org. Chem.* **1962**, *27*, 4666−4667.

(24) (a) Schlögl, K.; Fried, M.; Falk, H. *Monatsh. Chim.* **1964**, *95*, 576−597. (b) Abiko, A., Wang, G.-Q. *J. Org. Chem.* **1996**, *61*, 2264−2265.

(25) Iftime, G.; Daran, J.-C.; Manoury, E.; Balavoine, G. G. A. *Organometallics* **1996**, *15*, 4808−4815.

Scheme 1

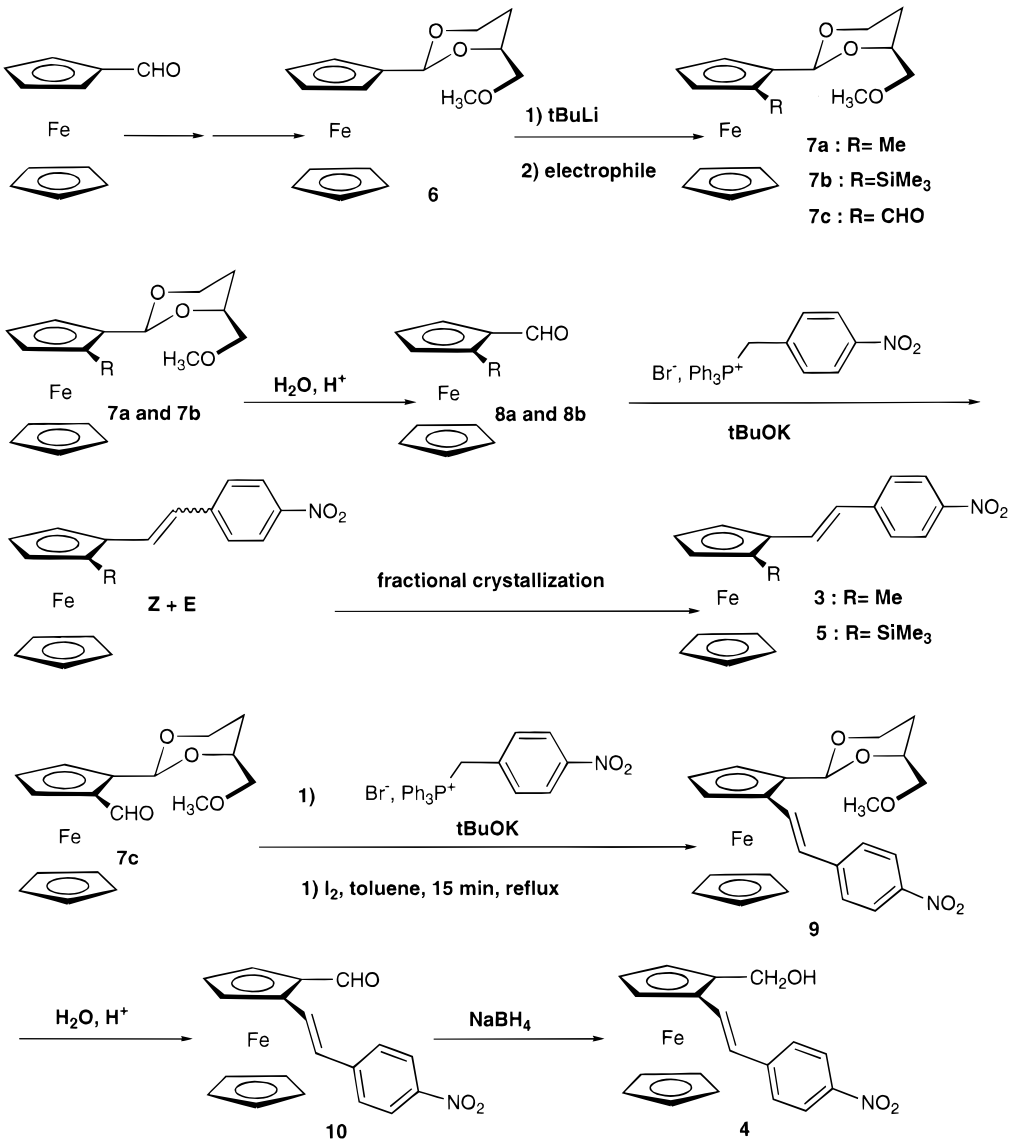

then the solution was kept at reflux for another 2 h. After the mixture was cooled back to room temperature, a solution of aldehyde in dry toluene (40 mmol L^{-1}) was added and the solution was warmed again. Within 1 h, 6 mL of toluene was removed by distillation. Then the solution was kept at reflux for another 2 h. After the solution was cooled to room temperature, the organic phase was extracted with methylene chloride and then washed with brine and dried on sodium sulfate and the solvents were evaporated under reduced pressure. The products were purified by flash chromatography on silica gel. For **3** and **5**, pure *E* isomers were obtained by fractional crystallization in cooled pentane. For **9**, the *E* isomer was isolated after an isomerization with I_2 (see below).

(*R*)-((*E*)-2-(4-Nitrophenyl)ethenyl)methylferrocene 3. ^{1}H NMR ($CDCl_3$; δ (ppm)): 8.18 (d, J = 8.8 Hz, 2H, C_6H_4); 7.54 (d, J = 8.8 Hz, 2H, C_6H_4); 7.19 (d, J = 16.1 Hz, 1H, vinyl); 6.74 (d, J = 16.1 Hz, 1H, vinyl); 4.53 (m, 1H, C_5H_3); 4.30 (m, 1H, C_5H_3); 4.27 (t, J = 2.5 Hz, 1H, C_5H_3); 4.07 (s, 5H, C_5H_5); 2.14 (s, 3H, CH_3). ^{13}C NMR ($CDCl_3$; δ (ppm)): 145.9 (C_6H_4); 144.6 (C_6H_4); 131.7 (vinyl); 125.8 (C_6H_4); 124.2 (C_6H_4); 123.6 (vinyl); 84.2 (C_5H_3); 80.4 (C_5H_3); 71.7 (C_5H_3); 69.9 (C_5H_5); 67.9 (C_5H_3); 64.8 (C_5H_3); 13.6 (CH_3). GC-MS (IE, 70 eV; *m/e*): 348 (M + 1, 21%); 347 (M, 100%); 301 (24%); 179 (12%); 178 (11%). $[\alpha]_D$ = +1625 ($CHCl_3$, c = 0.004). Anal. Calcd for $C_{19}H_{17}FeNO_2$: C, 65.71; H, 4.89; N, 4.03. Found: C, 65.15; H, 4.73; N, 4.12.

(*S*)-((*E*)-2-(4-Nitrophenyl)ethenyl)(trimethylsilyl)-ferrocene 5. ^{1}H NMR ($CDCl_3$; δ (ppm)): 8.17 (d, J = 8.8 Hz, 2H, C_6H_4); 7.49 (d, J = 8.8 Hz, 2H, C_6H_4); 7.22 (d, J = 16.0 Hz, 1H, vinyl); 6.73 (d, J = 16.0 Hz, 1H, vinyl); 4.81 (m, 1H, C_5H_3); 4.54 (t, J = 2.4 Hz, 1H, C_5H_3); 4.30 (dd, J = 2.4 and 1.2 Hz, 1H, C_5H_3); 4.16 (s, 5H, C_5H_5); 0.38 (s, 9H, $SiMe_3$). ^{13}C NMR ($CDCl_3$; δ (ppm)): 145.8 (C_6H_4); 144.4 (C_6H_4); 133.4 (vinyl); 125.7 (C_6H_4); 124.1 (C_6H_4); 123.9 (vinyl); 86.5 (C_5H_3); 76.1 (C_5H_3); 73.4 (C_5H_3); 72.0 (C_5H_3); 69.4 (C_5H_5); 68.0 (C_5H_3); 0.7 ($SiMe_3$). $[\alpha]_D$ = +1392 ($CHCl_3$, c = 0.016). Anal. Calcd for $C_{21}H_{23}FeNO_2Si$: C, 62.22; H, 5.68; N, 3.46. Found: C, 62.89; H, 5.14; N, 3.76.

Isomerization Reaction. Into a one-necked round-bottom flask equipped with a condenser were dissolved the compounds **9** (*Z* + *E*; 170 mg, 0.37 mmol) in toluene (concentration 1.5 10^{-2} mol L^{-1}) and I_2 (10 mg, 0.1 equiv). The system was purged with argon, and the mixture was warmed to toluene reflux for 15 min. After it was cooled back to room temperature, the mixture was extracted with methylene chloride, washed with a sodium thiosulfate solution (c = 2 mol L^{-1}) and then with brine, dried on sodium sulfate, and evaporated. After flash chromatography on silica gel, 160 mg (95%) of the pure (*E*)-**9** was isolated.

(2*S*,4*S*,R_{Fc})-4-(Methoxymethyl)-2-(((*E*)-2-(4-nitrophenyl)-ethenyl)ferrocenyl)-1,3-dioxane 9. ^{1}H NMR ($CDCl_3$; δ

(ppm)): 8.18 (d, J = 8.8 Hz, 2H, C_6H_4); 7.55 (d, J = 8.8 Hz, 2H, C_6H_4); 7.43 (d, J = 16.2 Hz, 1H, vinyl); 6.79 (d, J = 16.2 Hz, 1H, vinyl); 5.58 (s, 1H, O−CH−O); 4.56 (m, 2H, C_5H_3); 4.32 (t, J = 2.5 Hz, 1H, C_5H_3); 4.30 (dd, J = 12.0 and 5.1 Hz, 1H, CH−O); 4.16 (s, 5H, C_5H_5); 4.07 (m, 1H, CH−O); 3.99 (dd, J = 12.0 and 2.5 Hz, 1H, CH−O); 3.55 (dd, AB, J = 10.3 and 6.2 Hz, 1H, CH_2−OCH_3); 3.47 (dd, AB, J = 10.3 and 4.3 Hz, 1H, CH_2−OCH_3); 3.41 (s, 3H, OCH_3); 1.87 (qd, J = 12.0 and 5.1 Hz, 1H, CH); 1.52 (dd, J = 13.0 and 1.1 Hz, 1H, CH). ^{13}C NMR ($CDCl_3$; δ (ppm)): 145.6 (C_6H_4); 144.7 (C_6H_4); 132.1 (vinyl); 125.9 (C_6H_4); 124.2 (vinyl); 123.9 (C_6H_4); 99.9 (O−CH−O); 84.5 (C_5H_3); 80.3 (C_5H_3); 76.5; 75.4; 70.1 (C_5H_5); 69.4; 68.5; 66.9; 66.7; 59.2 (OCH_3); 27.4 (CH). $[\alpha]_D$ = −795 ($CHCl_3$, c = 0.003). Anal. Calcd for $C_{24}H_{25}FeO_2N$: C, 62.20; H, 5.40; N, 3.02. Found: C, 62.21; H, 5.43; N, 3.00.

(*R*)-(((*E*)-2-(4-Nitrophenyl)ethenyl)ferrocenecarboxaldehyde (10). Yield = 92%. ^{1}H NMR ($CDCl_3$; δ (ppm)): 10.11 (s, 1H, CHO); 8.14 (d, J = 8.8 Hz, 2H, C_6H_4); 7.70 (d, J = 16.3 Hz, 1H, vinyl); 7.56 (d, J = 8.8 Hz, 2H, C_6H_4); 6.87 (d, J = 16.3 Hz, 1H, vinyl); 5.05 (m, 1H, C_5H_3); 4.87 (m, 1H, C_5H_3); 4.72 (t, J = 2.6 Hz, C_5H_3); 4.25 (s, 5H, C_5H_5).^{13}C NMR ($CDCl_3$; δ (ppm)): 193.5 (CHO); 146.1 (C_6H_4); 143.7 (C_6H_4); 129.9 (vinyl); 126.3 (C_6H_4); 126.2 (vinyl); 124.0 (C_6H_4); 83.6 (C_5H_3); 77.2 (C_5H_3); 73.5 (C_5H_3); 73.3 (C_5H_3); 71.0 (C_5H_5); 70.5 (C_5H_3). $[\alpha]_D$ = −1350 ($CHCl_3$, c = 0.02). IR (KBr pellet): 1674 cm^{-1} (CHO). Anal. Calcd for $C_{19}H_{15}FeNO_3$: C, 63.16; H, 4.16; N, 3.88. Found: C, 64.92; H, 4.70; N, 2.80.

(*R*)-((*E*)-2-(4-Nitrophenyl)ethenyl)(hydroxymethyl)ferrocene (4). Yield = 88%. ^{1}H NMR ($CDCl_3$; δ (ppm)): 8.14 (d, J = 8.7 Hz, 2H, C_6H_4); 7.52 (d, J = 8.7 Hz, 2H, C_6H_4); 7.20 (d, J = 16.1 Hz, 1H, vinyl); 6.79 (d, J = 16.1 Hz, 1H, vinyl); 4.70 (m, 1H, C_5H_3); 4.66 (d, AB, J = 12.2 Hz, 1H, CH_2); 4.59 (d, AB, J = 12.2 Hz, 1H, CH_2); 4.51 (dd, J = 2.5 and 1.4 Hz, 1H, C_5H_3); 4.44 (t, J = 2.5 Hz, 1H, C_5H_3); 4.14 (s, 5H, C_5H_5); 1.92 (br s, 1H, OH). ^{13}C NMR ($CDCl_3$; δ (ppm)): 146.0 (C_6H_4); 144.3 (C_6H_4); 130.6 (vinyl); 126.1 (C_6H_4); 124.8 (vinyl); 124.2 (C_6H_4); 86.9 (C_5H_3); 81.2 (C_5H_3); 71.2 (C_5H_3); 69.7 (C_5H_5); 69.0 (C_5H_3); 68.8 (C_5H_3); 59.4 (CH_2). $[\alpha]_D$ = −940 ($CHCl_3$, c = 0.005). Anal. Calcd for $C_{19}H_{17}FeNO_3$: C, 62.81; H, 4.68; N, 3.86. Found: C, 63.37; H, 5.37; N, 3.48.

X-ray Crystal Structure Determination. Crystals suitable for X-ray analysis were obtained by slow diffusion of hexane into a dichloromethane solution of the studied compound. For the three compounds, data were collected at room temperature on an Enraf-Nonius CAD4 diffractometer equipped with a graphite oriented monochromator utilizing Mo Kα radiation (λ = 0.710 73 Å). The final unit cell parameters were obtained by the least-squares refinement of the setting angles of 25 reflections that had been accurately centered on the diffractometer. Only statistical fluctuations were observed in the intensity monitors over the course of the data collections.

The three structures were solved by direct methods (SIR92[26]) and refined by least-squares procedures on F. All H atoms attached to carbon were introduced in calculation in idealized positions (d(CH) = 0.96 Å), and their atomic coordinates were recalculated after each cycle. They were given isotropic thermal parameters 20% higher than those of the carbon to which they are attached. Least-squares refinements were carried out by minimizing the function $\sum w(|F_o| - |F_c|)^2$, where F_o and F_c are the observed and calculated structure factors. The weighting scheme used in the last refinement cycles was $w = w'[1 - \{\Delta F/6\sigma(F_o)\}^2]^2$, where $w' = 1/\sum_1^n A_r T_r(x)$ with three coefficients A_r for the Chebyshev polynomial $A_r T_r(x)$, where x was F_c/F_c(max).[28] Models reached convergence with $R = \sum(||F_o| - |F_d||)/\sum(|F_o|)$ and $R_w = [\sum w(|F_o| - |F_c|)^2/\sum w(F_o)^2]^{1/2}$, having values listed in Table 1.

Table 1. Crystal Data

	3	4	5
formula	$C_{19}H_{17}O_2NFe$	$C_{19}H_{17}O_3NFe$	$C_{21}H_{23}O_2NSiFe$
fw (g)	347.20	363.20	405.35
shape (color)	flat box (dark red)	needle (dark red)	box (dark red)
cryst syst	orthorhombic	monoclinic	monoclinic
space group	$P2_12_12_1$	$P2_1$	$P2_1$
a, Å	10.229(6)	7.621(2)	9.5719(7)
b, Å	11.485(2)	10.879(1)	11.741(1)
c, Å	27.629(7)	19.881(3)	9.575(2)
β, deg		91.95(2)	112.80(1)
V, Å^3	3246(2)	1647.5(5)	992.0(2)
Z	8	4	2
R	0.0429	0.0287	0.0231
R_w	0.0484	0.0325	0.0273
Flack param	0.02(3)	−0.02(3)	0.01(1)
GOF	0.980	1.168	1.074

Scheme 2

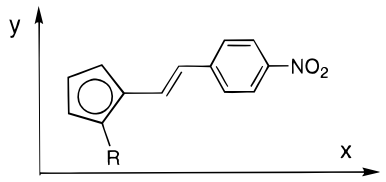

The calculations were carried out with the CRYSTALS package programs[29] running on a PC. Full crystal data, fractional atomic coordinates, anisotropic thermal parameters for non-hydrogen atoms, atomic coordinates for H atoms, and all bond lengths and bond angles have been deposited at the Cambridge Crystallographic Data Center.

Theoretical Methods. The all-valence INDO/S (intermediate neglect of differential overlap) formalism,[30] in connection with the sum over excited particle hole states (SOS) formalism, was employed.[22c] Details of the computationally efficient ZINDO-SOS-based method for describing second-order molecular optical nonlinearities have been reported elsewhere.[21] Standard parameters and basis functions were used.[30] In the present approach, the closed-shell restricted Hartree−Fock (RHF) formalism was adopted. The monoexcited configuration interaction (CIS) approximation was employed to describe the excited states. In all calculations, the lowest 180 and 300 (for the monomers and dimers, respectively) energy transitions between SCF and CIS electronic configurations were chosen to undergo CI mixing and were included in the SOS. This SOS truncation was found to be sufficient for complete convergence of the second-order response in all cases considered. All calculations were performed using the ZINDO program[21] implemented on an IBM ES/9000 system.

Metrical parameters used for the calculations were taken from present X-ray crystal structure data (vide infra). Each monomer was oriented so that the charge transfer axis is approximately along the x axis (see Scheme 2). Calculations on dimers were performed on the basis of X-ray crystal packing of the unit cell in which the first unit was oriented as in the monomer for the methyl derivative, while for the $SiMe_3$ derivative dimer the molecules were oriented as in the crystal cell, i.e., with the 2-fold axis along the y axis.

NLO Measurements. Powder Efficiencies. The measurements of second-harmonic generation (SHG) intensity were carried out by the Kurtz−Perry powder technique,[19] using a nanosecond Nd-YAG pulsed (10 Hz) laser operating at λ =

(26) Altomare, A.; Burla, M. C.; Camalli, M.; Cascarano, G.; Giacovazzo, C.; Guagliardi, A.; Polidori, G. *J. Appl. Crystallogr.* **1994**, *27*, 435.
(27) Flack, H. *Acta Crystallogr.* **1983**, *A39*, 876−881.
(28) Prince, E. *Mathematical Techniques in Crystallography*; Springer-Verlag: Berlin, 1982.
(29) Watkin, D. J.; Prout, C. K.; Carruthers, J. R.; Betteridge, P. W. CRYSTALS Issue 10; Chemical Crystallography Laboratory, University of Oxford, Oxford, U.K.,1996.
(30) (a) Zerner, M.; Loew, G.; Kirchner, R.; Mueller-Westerhoff, U. *J. Am. Chem. Soc.* **1980**, *102*, 589−599. (b) Anderson, W. P.; Edwards, D.; Zerner, M. C. *Inorg. Chem.* **1986**, *25*, 2728−2732.

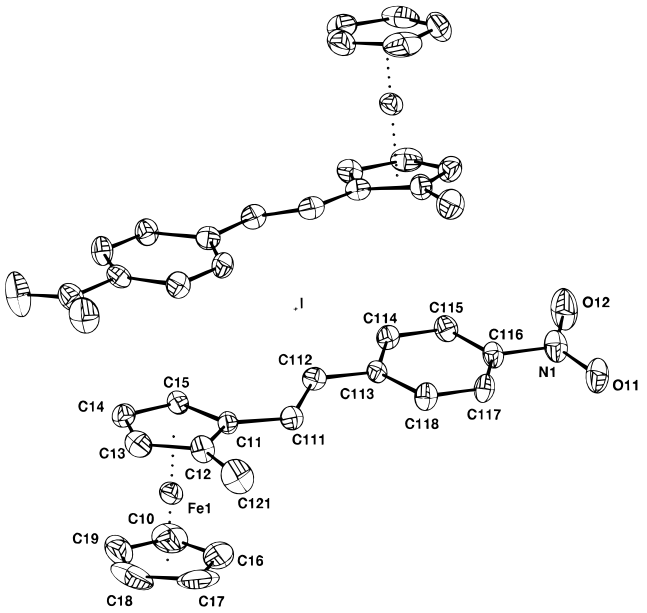

Figure 1. View of the asymmetric unit with the two independent molecules related by the pseudo inversion center (I) for compound **3**. Ellipsoids are drawn at 30% probability.

Table 2. Synthesis of Chromophores by the Wittig Reaction

compd	isolated yield, %	*E*/*Z* ratio
3	69	2.9/1
9	97	2.6/1
5	79	3.1/1

1.064 μm. The outgoing Stokes-shifted radiation at 1.907 μm, generated by the Raman effect in a hydrogen cell, was used as the fundamental beam for second-harmonic generation. The SHG signal was detected by a photomultiplier and read on an ultrafast Tektronic 7834 oscilloscope. Samples were calibrated microcrystalline powders obtained by grinding in the range 50−80 μm and put between two glass plates. The recorded efficiencies were expressed versus that of powdered (50−80 μm) urea.

EFISH Measurements. The principle of the electric-field-induced second-harmonic (EFISH) technique is reported elsewhere.[20,31] The data were recorded using the 1.907 μm incident laser beam generated as described above. The laser delivered pulses of 10 ns. The compounds were dissolved in dioxane at various concentrations (0 to 5×10^{-3} mol L^{-1}). The centrosymmetry of the solution was broken by dipolar orientation of the chromophores with a high-voltage pulse (around 5 kV applied on 2 mm during 5 μs) synchronized with the laser pulse. Calibration of the cell was made by monitoring the SHG generated by a series of 2-methyl-4-nitroaniline (MNA) in dioxane. The dipole moments were measured independently by a classical method based on the Guggenheim theory.[32] Further details of the experimental methodology and data analysis are reported elsewhere.[31]

Results

Synthesis. The aldehydes **8a**,**b** and **7c** have been successfully synthesized by the method described by Kagan et al. in an enantiomerically pure form.[18] By a Wittig reaction,[33] the chromophores **3**, **5,** and **9** were efficiently obtained, but as a mixture of diastereoisomers (see Table 2). The isomers (*Z* or *E*) of both **3** and **5** could not be separated by flash chromatography on silica gel; however, a fractional crystallization in cold pentane allowed the isolation of pure (*E*)-**3** and pure **(*E*)-5**.

The isomerization of olefins in the presence of I_2 have been largely used to convert a mixture of *Z* and *E* olefins into pure *E* isomer.[34] In the case of **9**, if the temperature of the reaction was limited to 110 °C (toluene reflux) and if the reaction time was only 15 min, this method gave excellent yields of pure (*E*)-**9** (isolated yield 95%). The acidic hydrolysis[18a] of **9** gave **10** with a very good yield (isolated yield 92%). A reduction by $NaBH_4$[25] yielded the desired alcohol **4** (isolated yield 88%).

Description of Structures. An X-ray crystallographic study for each of the three compounds **3**−**5** was carried out. Crystal data are given in Table 1, whereas Figures 1−5 show CAMERON[35] views of the molecules. For all three structures, bonding parameters for the ferrocene unit fall in the expected range.[36]

All three complexes are enantiomerically pure and therefore crystallize in a noncentrosymmetric space group. The absolute configuration for each structure was determined by careful examination of the sensitive reflections and refining Flack's enantiopole parameter[27]

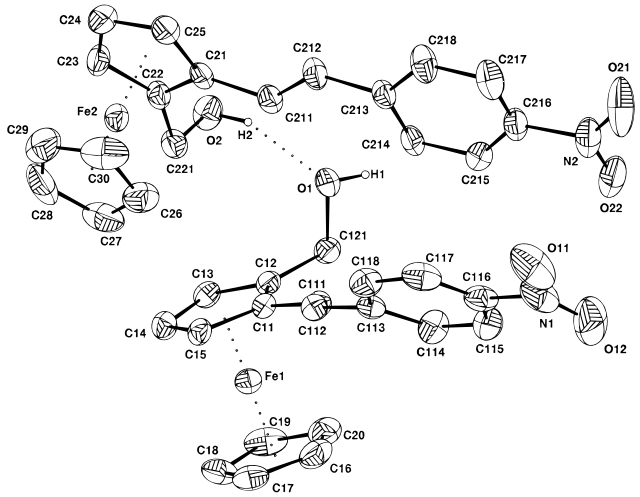

Figure 2. View of the asymmetric unit with the two molecules linked through H bond for compound **4**. Ellipsoids are drawn at 30% probability.

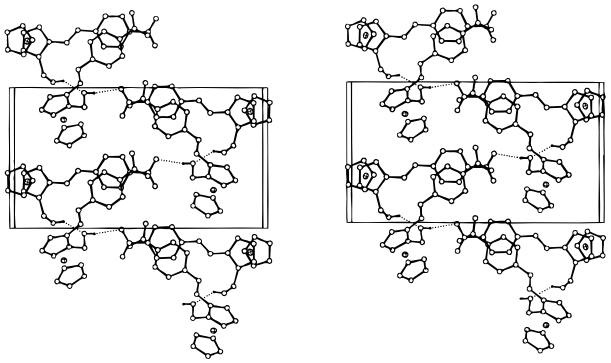

Figure 3. Stereoview of the stacking for **4** showing the H-bond network around the 2-fold screw axis.

(31) Maltey, I.; Delaire, J. A.; Nakatani, K.; Wang, P.; Shi, X.; Wu, S. *Adv. Mater. Opt. Electron.* **1996**, *6*, 233−238.
(32) Guggenheim, E. A. *Trans. Faraday Soc.* **1949**, *45*, 714−720.
(33) Fitjer, L.; Quebeck, U. *Synth. Commun.* **1985**, *15*, 855−864.
(34) Sonnet, P. E. *Tetrahedron* **1980**, *36*, 557−604.
(35) Watkin, D. J.; Prout, C. K.; Pearce, L. J. CAMERON; Chemical Crystallography Laboratory, University of Oxford, Oxford, U.K., 1996.

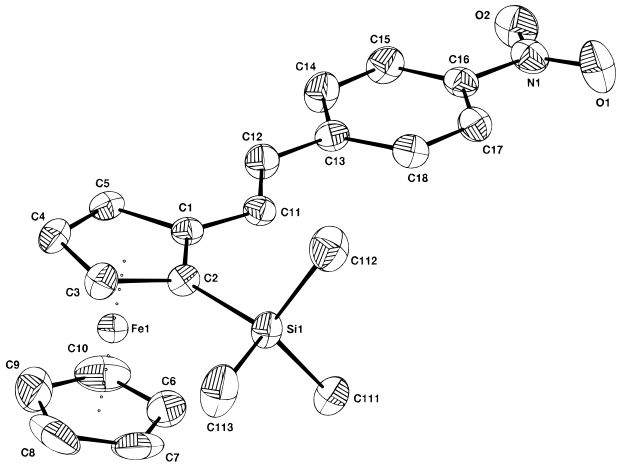

Figure 4. Molecular view of compound **5**. Ellipsoids are drawn at 30% probability.

x, which is defined as

$$F_o^2 = (1 - x)F(h)^2 + xF(-h)^2$$

It is then the fractional contribution of $F(-h)$ to the observed structure amplitude, and it is sensitive to the polarity of the structure. The *x* values for each structure are given in Table 1; they agree with the absolute configuration expected from the synthetic route.

Compound **3** crystallizes in the orthorhombic space group $P2_12_12_1$, with two independent molecules in the asymmetric unit. No significant differences in bonding parameters between these two molecules were found. The nitrophenyl groups are nearly coplanar with the corresponding ferrocene ring, the dihedral angle between these planes is 7.6 and 10.8° for molecule 1 and molecule 2, respectively.

The most interesting and, in view of the NLO properties, the most decisive feature revealed by the crystal structure is the relative position of these two molecules. As illustrated in Figure 1, they are related by a pseudo inversion center. The unit cell thus contains four pairs of molecules in an almost perfect antiparallel arrangement. The material is almost centrosymmetrical. A similar situation was recently reported for some related vinylferrocene complexes.[37,25]

Compound **4** crystallizes in the monoclinic space group $P2_1$ with again two molecules in the asymmetric unit. However, in that case, the two molecules are not independent, they are indeed related by hydrogen bonding between the two hydroxyl groups (O(2)−H(2)- - - O(1), 0.85(5) Å, 2.06(5) Å, 145(5)°). Such a hydrogen bond induces a roughly parallel arrangement of the two molecules, as shown by the 38° angle observed between the two vectors linking the centroid of the Cp and the nitrogen of the NO_2 group for each molecule. However, the unit cell shows a roughly pairwise antiparallel orientation of these molecules around the 2-fold axis.

It is worth pointing out that there is also a hydrogen bonding interaction between the O(1)−H(1) group of molecule 1 and the O(21) atom of the nitro group of the 2_1 symmetry-related $(1 - x, y - {}^1/_2, 1 - z)$ molecule 2. This hydrogen-bonding interaction might be responsible for the strong distortion observed in molecule 1, where the dihedral angle between the Cp and the phenyl ring is 48.1°, whereas the 10.1° observed in molecule 2 is identical with the values observed in compound **3**. For molecule 1, the observed molecular twisting in the crystal may be of prime importance when the NLO responses are compared in the solid state and in solution. This hydrogen-bonding interaction results also in the buildup of a two-dimensional network which develops as a flattened left-handed helix around the 2-fold axis (Figure 3).

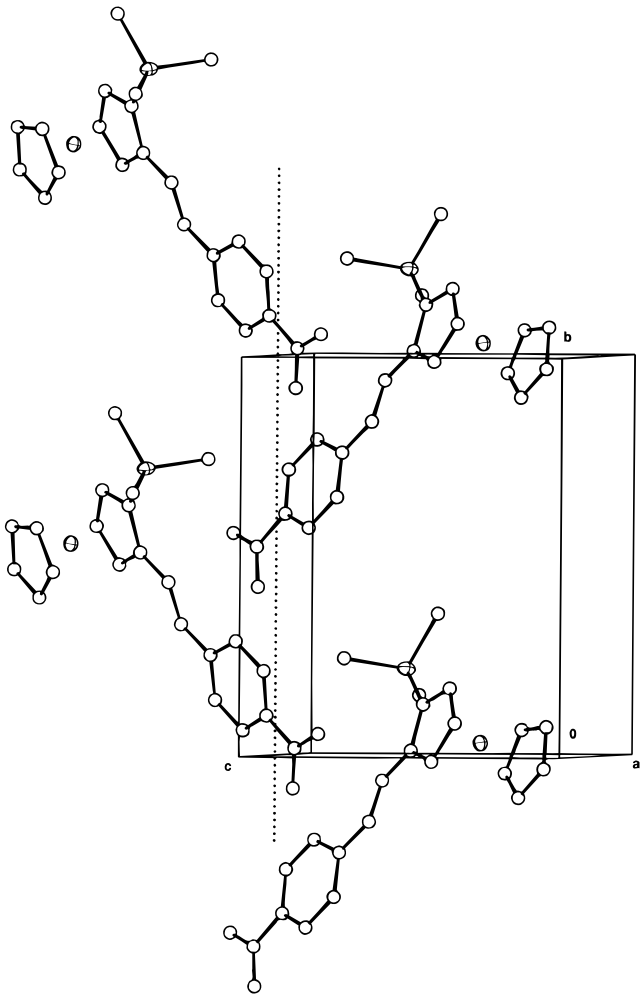

Figure 5. Packing of molecules **5** around the 2_1 axis.

Compound **5** crystallizes in the monoclinic space group $P2_1$ with surprisingly only one molecule in the asymmetric unit. The phenyl ring is found to only slightly deviate from coplanarity with the cyclopentadienyl ring (8.2°), as already observed for **3** (Figure 4). The molecules pack in the crystal in such a way that the vector parallel to the donor−acceptor charge-transfer axis represented by the direction between the centroid of the Cp ring and the nitro group make a 45.4° angle with the 2-fold screw axis (Figure 5).

Molecular Hyperpolarizabilities. The purpose of the following section is to study the influence of the substitution on the second-order NLO response of the chromophores. The noncentrosymmetry of the solution being induced by dipolar orientation of the chro-

(36) The crystallographic data (atomic coordinates and bonding parameters) have been placed in the Supporting Information. This is because the main goal of the X-ray diffraction was to (a) confirm the structure of compounds **3**−**5** and (b) clarify the relative orientation of the molecules in the unit cell. Further, the molecular structures do not present any exceptional features.

(37) Togni, A.; Rihs, G. *Organometallics* **1993**, *12*, 3368−3372.

Table 3. Computed Dipole Moment and Second-Order NLO Response at 1.907 μm for Ferrocenyl Monomer and Dimer Complexes (μ in D, β in 10^{-30} cm^5 esu^{-1})

	dipole moment				hyperpolarizability; principal tensor components							
compd	μ_x	μ_y	μ_z	μ_{tot}	$\beta_{0,vec}$[a]	β_{vec}	β_{xxx}	β_{yyy}	β_{yxx}	$\beta_{xxy}=\beta_{xyx}$	β_{yzz}	$\beta_{zyz}=\beta_{zzy}$
2	7.6	0.8	0.2	7.6	23.4	29.6	30.5					
3 (monomer)	7.7	1.0	0.4	7.8	21.3	26.8	27.3					
3 (dimer)	0.4	1.8	0.1	1.8		8.3	7.1					
4 (molecule 1)	6.7	2.0	1.0	7.1	14.6	18.0	19.6					
4 (molecule 2)	6.1	2.8	0.2	6.8	17.2	21.2	23.0					
5 (monomer)	7.7	1.2	0.2	7.8	24.9	31.5	32.4					
5 (dimer)	−0.02	11.0	−0.02	11.0		40.1		14.6	13.4	13.5	11.9	11.9

[a] $\beta_{0,vec}$ is the projection of β on the dipole moment calculated at zero frequency ($h\omega = 0.0$ eV).

Table 4. Experimental[a] and ZINDO-Derived Linear Optical Spectroscopic and Nonlinear Optical Response Parameters and Dipole Moment for Ferrocenyl Complexes

	λ_{max} (nm)		μ (D)		β_{vec}	
compd	exptl ($\epsilon \times 10^{-3}$)	calcd (f)	exptl	calcd	exptl	calcd
2	356 (18 300)	350 (0.84)	5.8	7.6	31	29.6
3	359 (17 600)	344 (0.81)	5.4	7.7	24	26.8
4 (molecule 1)	362 (12 900)	329 (0.72)	5.6	7.1	43	18.0
4 (molecule 2)	362 (12 900)	330 (0.89)	5.6	6.1	43	21.2
5	357 (20 000)	352 (0.84)	5.2	7.7	36	31.5

[a] Recorded in dioxane solution.

mophores by a pulse of high voltage, the square root of the signal obtained by EFISH is proportional to the dipole moment (μ) and to β_{vec}, the vector component of the β_{ijk} tensor along the dipole moment direction. The ZINDO-based NLO response of compounds **2**−**5** are gathered in Table 3. Calculations indicate that the principal dipole moment component (μ_x), and the largest hyperpolarizability tensor component (β_{xxx}), are almost parallel, i.e., along the donor−acceptor charge-transfer axis of the molecule, while the other hyperpolarizability tensor components are negligible (smaller than 4×10^{-30} esu). Thus, β_{vec} values are comparable to β_{xxx} for each chromophore. It can be observed that the large $SiMe_3$ substituent in **5** does not modify significantly the magnitude and orientation of the dipole moment.

The experimental and calculated relevant spectroscopic properties, hyperpolarizabilities (β_{vec}), and dipole moments (μ) of compounds **2**−**5** are summarized in Table 4. Except for compound **4**, which will be discussed below in more detail, the agreement between theory and experiment seems to be satisfactory. In particular, the nature of the substituent R seems to have only a slight effect on the NLO response of the molecules. A detailed analysis of the computational results indicates that the second-order NLO response of the present complexes is dominated in all instances by the intense lowest charge-transfer excitation, in which the metal acts as an electron donor and the NO_2 group as an acceptor. In such cases, the quadratic hyperpolarizability can be simply related to the two-state contribution,[38] as previously found for unsubstituted ferrocenyl complexes.[7b] In this model, β can be described in terms of a ground and a single excited state having charge-transfer character and is related to the energy of the optical transition (E), its oscillator strength (f), and the difference between ground and excited-state dipole moment ($\Delta\mu$) through the relation

$$\beta_{xxx} \propto f\Delta\mu/E^3$$

Therefore, the increasing β_{vec} values observed on passing from R = Me to R = H and $SiMe_3$ complexes can be directly related to the increasing CT character, hence greater $\Delta\mu$ values, and to the bathochromic shift of the β-determining CT transition (Table 5). The compositions of mixing coefficients of the CI expansion of the dominant excited state involved in the nonlinearities of **2**−**5** are reported in Table 5. It should be pointed out that the origin of the nonlinearity is similar for each compound and can be related to the 1→10 low-lying CT optical transition, principally involving the Fe 3d-based HOMO and the NO_2-based LUMO. As anticipated, the involvement of the R substituents in these orbitals is modest and, therefore, the electronic properties of each compound are similar.

The UV−visible optical absorption spectra of compounds **2**−**5** are reported in Figure 6. Compounds **2**, **3**, and **5** exhibit very similar features with a low lying transition around 500 nm and an intense charge-transfer transition (ϵ = 18 300, 17 600, and 20 000 M^{-1} cm^{-1}, for **2**, **3**, and **5**, respectively) around 350 nm. In accord with experimental data for compounds **2, 3,** and **5**, slight changes are predicted as far as the calculated λ_{max} and the intensity of lowest CT transition are concerned. For reasons which are probably related to molecule distortions in the crystals, experiment and calculations, based on atomic positions taken from the crystal structure, substantially disagree for compound **4**. In fact, in contrast with calculated data, the transition responsible for the NLO response of compound **4** exhibits the lowest intensity (ϵ = 12 900 mol^{-1}) in this family of ferrocenyl derivatives. In addition, the blue shift predicted by calculations (λ_{max} = 330 nm) is not observed experimentally. As already mentioned, the crystal structure of **4** reveals that the chromophores are embodied in diads through a hydrogen-bonding network. This proximity may induce steric hindrance and dipolar interaction, which might affect the overall electronic properties of the molecules in the solid state. No further investigations were carried out to assess this effect, which may partially account for the disagreement between theory and experiment.

Bulk Susceptibility. The SHG efficiencies of powder compounds **2**−**5** are reported in Table 6. Large differences, ranging from 0 to 6, 20, and 100, are observed in the powder efficiencies of compounds **2**, **3**, **4**, and **5**, respectively, although the molecular hyperpolarizabilities are quite similar. While compound **2** exhibits zero efficiency, as anticipated for a probably centrosymmetric crystal structure, the chiral compounds **3**, **4**, and **5**

(38) Oudar, J. L.; Chemla, J. *J. Chem. Phys.* **1977**, *66*, 2664−2668.

Table 5. Energy (λ_{max} in nm), Oscillator Strength (f), Dipole Moment Change between Ground and Excited States ($\Delta\mu$ in D), and Composition of the Dominant Excited State Involved in the Nonlinearity of Ferrocenyl Complexes

compd (R)	transition (λ_{max})	f	$\Delta\mu$	composition of CI expansion[a]
2 (H)	1→10 (350)	0.84	15.9	$0.56\chi_{54\rightarrow57} + 0.70\chi_{56\rightarrow57}$
3 (Me)	1→10 (344)	0.81	16.2	$0.60\chi_{57\rightarrow60} + 0.66\chi_{59\rightarrow60}$
4 (CH_2OH)				
molecule 1	1→10 (329)	0.72	16.0	$-0.63\chi_{60\rightarrow63} + -0.63\chi_{62\rightarrow63} + 0.24\chi_{68\rightarrow70}$
molecule 2	1→10 (330)	0.89	14.9	$0.56\chi_{60\rightarrow63} + 0.70\chi_{62\rightarrow63} + 0.22\chi_{62\rightarrow64}$
5 ($SiMe_3$)	1→10 (352)	0.84	16.2	$0.22\chi_{60\rightarrow69} + -0.58\chi_{66\rightarrow69} + 0.68\chi_{68\rightarrow70}$

[a] 56, 59, 62, and 68 are HOMO's for **2**, **3**, **4**, and **5**, respectively.

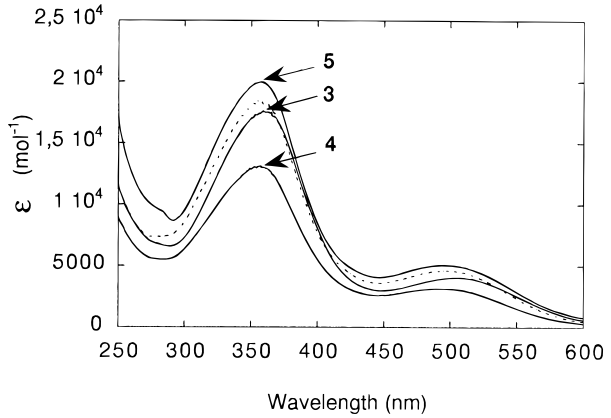

Figure 6. UV−visible optical absorption spectra of compounds **3**−**5** recorded in dioxane. The dotted line corresponds to the parent derivative **2**.

Table 6. Efficiencies versus Urea Recorded at 1.907 μm on Calibrated Samples in Relation to β_{vec} (in 10^{-30} cm^5 esu^{-1}) and the Evaluated Non-Zero Tensor Components $\chi_{IJK}^{(2)}$ (in cm^2 esu^{-1}) for Ferrocenyl Complexes

compd	efficiency (size, μm)	β_{xxx} (calcd)	tensor component of $\chi^{(2)}$ [a] $10^9 d_{YXX}$	$10^9 d_{YYY}$
2	0 (50−80)	30.5		
3	6 (50−80)	27.3		
4	20 (50−80)	19.6 (molecule 1)	8.93	6.28
5	100 (50−80) 90 (80−125) 80 (125−180)	32.4	22.7	21.9

[a] Space group $P2_1$ (compounds **4** and **5**). The calculation assumes $f_I^{2\omega} = f_J^{\omega} = f_k^{\omega} = 1$. $N = 1.21 \times 10^{21}$ and 2.02×10^{21} cm^{-3} for **4** and **5**, respectively.

exhibit sizable bulk nonlinearities. In particular, 100 times the efficiency of urea is one of the largest values reported for a ferrocene-based chromophore.[15]

It is well-known that chirality provides the synthetic chemist with a means of guaranteeing that crystallization of a pure enantiomer will occur in a noncentrosymmetrical space group. However, the fact that a molecule is optically pure does not guarantee that the molecular packing will be optimized for NLO effects. Therefore, the different SHG efficiencies recorded for the chiral derivatives **3**−**5** must necessarily be related to the different arrangements of the chromophores in the crystals.

The relations between microscopic and macroscopic second-order optical nonlinearities have been extensively investigated for any noncentrosymmetric crystal point group by Zyss[39] with the aim of founding optimized geometry. The hyperpolarizability tensor components (components β_{ijk} in the molecular frame) are related to the corresponding crystal quadratic nonlinearity $\chi^{(2)}$ (components d_{IJK} in the crystalline frame) through the relation

$$d_{IJK}(-2\omega;\omega,\omega) = Nf_I^{2\omega}f_J^{\omega}f_K^{\omega}\sum\cos(I,i)\cos(J,j)\cos(K,k)\,\beta_{ijk}$$

N is the number of chromophores per unit volume, and $f_I^{2\omega}$, f_J^{ω}, and f_K^{ω} are Lorentz local-field factors. The summation is performed over all molecules in the unit cell, and the cosine product terms represent the rotation from the molecular reference frame into the crystal frame.

Alternatively, the macroscopic second-order nonlinearity can be evaluated by means of the calculation of the effective hyperpolarizability of a molecular cluster representative of the crystal environment, such as the crystal unit cell. In this case, instead of the use of local field empirical factors, a reliable quantum chemical electronic structure formalism can be used to evaluate the interchromophore effects upon molecular packing.[40]

The situation encountered in the case of **3** can be readily analyzed by considering the calculated β value of the asymmetric unit cell, made of two chromophores embodied in an almost antiparallel molecular dipole arrangement. The natural trend for dipole cancellation (μ_{tot} = 1.8 D) results in an almost centrosymmetric packing structure, thus canceling most of the contribution of the largest β_{xxx} tensor component of each monomer (Table 3). Nevertheless, a small resulting net dipole moment is achieved along the y axis essentially due to the residual noncentrosymmetry of the two methyl groups. The almost vanishing β_{vec} of the asymmetric unit will result in a modest efficiency for any orientation.

The main modification introduced in the molecular structure of **4** is the presence of a hydroxy group. Chirality combined with hydrogen bonding has already been successfully used in designing molecular materials with high SHG efficiencies.[17] At first, the crystal structure of **4** seems to favor higher efficiencies. Due to hydrogen bonding, the deleterious trend for dipole cancellation is avoided in the asymmetric unit cell, where two chromophores are fairly well aligned (Figure 2). Before trying to rationalize the structure-efficiency relationship, it is of interest to note that the angle (θ) between the 2-fold axis (2_1) and the charge-transfer axis of one molecule (molecule 2) of the asymmetric unit of **4** is 86°, canceling most of the contribution of this

(39) Zyss, J.; Oudar, J. L. *Phys. Rev. A* **1982**, *26*, 2028−2048.
(40) Di Bella, S.; Ratner, M. A.; Marks, T. J. *J. Am. Chem. Soc.* **1992**, *114*, 5842−5849.

chromophore by 2_1 symmetry. θ is equal to 50° for the other molecule (molecule) present in the asymmetric unit (Figure 3). Therefore, it can be assumed that half of the chromophores contribute to an observable bulk nonlinearity of **4** ($N = 1.21 \times 10^{21}$ cm^{-3}).

The best alignment of present ferrocenyl derivatives in the crystal frame is achieved for compound **5**, where θ is equal to 45.4° for each chromophore unit (Figure 5). The calculation of the hyperpolarizability performed on the unit cell (Table 3, entry 5 (dimer)) indicates a total nonlinearity, β_{vec}, larger than that calculated for the monomer. As expected on the basis of the crystal packing, the resulting dipole and charge-transfer axis of the unit cell is oriented along the *b* axis. Therefore the largest β tensor component is β_{yyy}. In addition, various nonvanishing hyperpolarizability tensor components, in addition to the largest β_{yyy} tensor, are predicted. They bring about compound **5** with three-dimensional character. Interaction between the two ferrocenyl units in the dimer can be described in terms of small stabilizing dipole−dipole interactions. In fact, relevant involved MOs have only slightly distorted charge distribution and minimal contributions from the orbitals of the other subunit. The excited states may be characterized simply as a linear combination of monomer states. Consequently, the NLO response can be related to an almost independent contribution of each nearly unperturbed molecular subunit, resulting in a total nonlinearity larger than that of the monomer. In fact, a powder SHG efficiency substantially larger than that observed for **3** is achieved for **5**.

The Zyss model can be employed to qualitatively compare the efficiencies of compounds **4** and **5**, which crystallize in the same space group ($P2_1$). On the basis of the calculated data (Table 3), β has only one nonvanishing coefficient along the charge-transfer axis *x* of the molecule (namely β_{xxx}). In the space group $P2_1$, this model leads to these formulas, *X*, *Y*, and *Z* beiing the coordinates in the crystal frame:[17a]

$$d_{YXX} = N\beta_{xxx} \cos\theta \sin^2\theta$$

$$d_{YYY} = N\beta_{xxx} \cos^3\theta$$

All other components of the tensor are considered negligible (θ is defined as the angle between the main intramolecular charge-transfer axis 0_X and the 2-fold axis 0_Y of the crystal). These components have been calculated (Table 6). In compound **4**, only half of the chromophores are assumed to be SHG active ($\theta = 50°$, $N = 1.21 \times 10^{21}$ cm^{-3}), while every chromophore is active in compound **5** ($\theta = 45.5$, $N = 2.02 \times 10^{21}$ cm^{-3}). The data are consistent with a higher efficiency for compound **5**. The angular factor weighting β_{xxx} in the expression of d_{YXX} is maximized and is equal to 0.385 for $\theta = 54.74°$. According to theoretical analysis,[39] any phase-matching configuration emphasizing this coefficient is to be considered as highly desirable. Although the data reported in Table 6 indicate that compound **5** is probably not phase matchable (the efficiencies decrease with increasing grain size), the angular factor reaches 0.356, which means that compound **5** is nearly optimized for SHG properties.

Conclusion

We have reported on a series of new chiral enantiomerically pure ferrocene NLO chromophores. The investigation conducted using both experimental (EFISH) and theoretical (INDOS/CI-SOS) approaches revealed closely related molecular hyperpolarizabilities for all of them. In contrast, their SHG efficiencies lay in various ranges of magnitude by virtue of different molecular packings in the solid state.

The prediction of a crystal structure from the molecular structure is still an unsolved problem;[41−43] nevertheless, we have demonstrated that chirality could be successfully used to reach a high level of solid-state NLO efficiency. Indeed, some chiral ferrocenyl chromophores have been obtained in a enantiomerically enriched form[25,37,44,45] and have, in some cases, sizable SHG efficiencies (χ^2 up to 17.5 times the value for urea);[44] however, **5** is, to the best of our knowledge, the chiral organometallic chromophore with the best bulk susceptibility ever reported ($\chi^2 = 100$ times the value for urea)!

Acknowledgment. We gratefully acknowledge financial support from the Centre National de la Recherche Scientifique (CNRS), and G.I. thanks the Ministère des Affaires Etrangères for a Doctoral Fellowship. We thank Olivier Guilbaud and Jean-François Delouin (ENS Cachan) for assistance in EFISH measurements and the Laboratoire de Recherche Thomson-CSF (Orsay) for the use of a dipole meter.

Supporting Information Available: Further details of the structure determination, including tables of atomic coordinates, bond distances and angles, and thermal parameters (13 pages). Ordering information is given on any current masthead page.

OM980826Y

(41) Gavezzoti, A. *Acc. Chem. Res.* **1994**, *27*, 309−314.
(42) Desiraju, G. R. *Angew. Chem., Int. Ed. Engl.* **1995**, *34*, 2311−2327.
(43) Wolff, J. J. *Angew. Chem., Int. Ed. Engl.* **1996**, *35*, 2195−2197.
(44) Bunting, H. E.; Green, M. L. H.; Marder, S. R.; Bloor, D.; Kolinsky, P. V.; Jones, R. J. *Polyhedron* **1992**, *11*, 1489−1499.
(45) Colbert, M. C. B.; Lewis, J.; Long, N. J.; Raithby, P. R.; Bloor, D. A.; Cross, G. H. *J. Organomet. Chem.* **1997**, *531*, 183−190.